Electronic Supplementary Information

<mark>**Enhanced Water Stability of MOFs via Multiple Hydrogen Bonds and the Application in Water Harvesting**</mark>

Yi-Chao Wang,[a] Mo-Han Chen,[a] Zi-Wen Fan,[a] Yue Wang,[a] Cai-Xiang Huang,[a] Hui-Fang Wang,[a] Jian-Ping Lang,*[ab] Zheng Niu*[a]*

[a] College of Chemistry, Chemical Engineering and Materials Science, Soochow University, Suzhou, Jiangsu, 215127.

[b] State Key Laboratory of Organometallic Chemistry, Shanghai Institute of Organic Chemistry, Chinese Academy of Sciences, Shanghai 200032.

zhengniu@suda.edu.cn;

jplang@suda.edu.cn;

wanghf@suda.edu.cn.

Table of Contents

1. General procedures

All starting materials and solvents were purchased from commercial sources and used as supplied without additional purification unless otherwise mentioned.

NMR measurements

Liquid NMR spectra were recorded on Bruker AVANCE Ⅲ HD (400MHz) at room temperature and referenced to the residual protonated solvent for NMR spectra. Proton chemical shift δ H = 2.50 (DMSO-d_6) ppm is reported relative to the solvent residual peak.

PXRD measurements

Powder X-ray diffraction (PXRD) patterns were acquired on a PANalytical X'Pert PRO MPD system (PW3040/60) using Cu Kα radiation (λ = 1.5406 Å) from 3 ° to 50 ° with a scanning step size of 0.02 °.

SEM measurements

Scanning electron microscopy (SEM) images were obtained with a HITACHIS-4700 cold field emission scanning electron microscope operating at 10-30 kV.

Gas adsorption measurements

The sample was degassed under high vacuum (< 5 μmHg) for 12 hours prior to sorption measurement by Micromeritics ASAP 2020 surface area and Porosity Analyzer. The apparent surface areas were determined from the nitrogen adsorption isotherm collected at 77 K by applying the Brunauer-Emmett-Teller (BET) models. Pore-size distributions were obtained from DFT calculations using a carbon slit-pore model with a N_2 kernel.

TGA analysis

Thermogravimetric analysis (TGA) was performed on TGA 4000 PerkinElmer Co., Ltd. ranging from 0 to 800 ℃ at the heating rate of 10 ℃/min under continuous nitrogen flow.

Water vapor adsorption measurements

Water vapor adsorption isotherms as well as all water cycling experiments were measured by a gravimetric method. For cyclic water vapor sorption measurements, samples were regenerated under vacuum at 298 K for 8 hours. All water analyses were performed using a programmable water bath with a recirculating chiller.

2. Synthesis

2.1 Synthesis of 2,4,6-tris(3,5-dicarboxylphenylamino)-1,3,5-triazine (H$_6$TDPAT)

H$_6$TDPAT was prepared according to the literature.[S1] 5-aminoisophthalic acid (15.2 g, 0.084 mol), NaOH (5.36 g, 134 mmol) and NaHCO$_3$ (8.74 g, 104 mmol) were added to 140 mL H$_2$O and stirred at 0 ℃ for 30 minutes. Then, a solution of cyanuric chloride (3.68 g, 20 mmol) in 1,4-dioxane (70 mL) was added dropwise with stirring. The mixture was heated under reflux at 100 ℃ for 24 hours. After cooling to room temperature, the resulting solution was adjusted to pH = 2 with HCl solution. The solid was collected by filtration, washed with deionized water several times, and dried to obtain H$_6$TDPAT (11.55 g, yield: 94%). ^{1}H NMR (DMSO-d$_6$, 400 MHz): δ = 8.12 (3H), 8.47 (6H), 9.67 (3H), 13.0 (6H) ppm.

2.2 Synthesis of HKUST-1

HKUST-1 was solvothermally synthesized following the modified procedure reported previously.[S2] Copper chloride (0.23 g, 1.72 mmol) was dissolved in methanol (40 mL) and 0.5 mL of DMF was added; 1,3,5-benzenetricarboxylic acid (0.42 g, 2 mmol) was dissolved in methanol (40 mL) and 0.04 mL of concentrated hydrochloric acid was added. A solution of copper chloride was added to a solution of 1,3,5-benzenetricarboxylic acid. The mixture was stirred for 10 minutes and transferred to a 20 mL glass vial, which was then placed in an oven at 80 ℃ for 5 days. Blue crystals were collected.

2.3 Synthesis of [(Cu$_3$(TDPAT)(H$_2$O)$_3$)·10H$_2$O·5DMA] (Cu-TDPAT-DMA)

Cu-TDPAT-DMA was prepared according to the literature with minor modifications.[S1] 0.009 g (0.0147 mmol) of H$_6$TDPAT and 0.0492 g (0.204 mmol) of Cu(NO$_3$)$_2$·3H$_2$O were dissolved in 0.6 mL N,N-Dimethylacetamide (DMA), 0.6 mL Dimethyl sulfoxide (DMSO) and 0.03 mL of H$_2$O. Subsequently, 0.35 mL HBF$_4$ was added to the mixture, which was then transferred to a 5 mL glass vial. The mixture was heated at 85 ℃ for 3 days. After cooling down to room temperature, blue octahedral crystals were filtered and washed with DMA.

2.4 Preparation of anhydrous [(Cu$_3$(TDPAT)] (Cu-TDPAT)

The crystals of Cu-TDPAT-DMA were soaked in anhydrous methanol for 3 days with fresh methanol 9 times. Then, the crystals were vacuumed at room temperature till the pressure below to 5 μmHg, the temperature was increased to 120 °C and vacuum for 12 hours. Consequently, the dark purple crystal of anhydrous Cu-TDPAT was obtained.

2.5 Preparation of hydrated Cu-TDPAT

The crystals of Cu-TDPAT-DMA were soaked in anhydrous methanol for 3 days with fresh methanol 9 times. Then, the crystals were vacuumed at room temperature till the pressure below to 5 μmHg, the temperature was increased to 120 ℃ and vacuum for 8 hours. Consequently, the dark purple crystal of hydrated Cu-TDPAT was obtained. The crystals were picked out and covered with the degassed oil in the glove box after 1 hour for single crystal X-ray diffraction measurements.

2.6 Preparation of water-loaded Cu-TDPAT at 4.12 $\times 10^{-3}$ bar (Cu-TDPAT-H$_2$O-1)

The selected anhydrous Cu-TDPAT was filled into a glass tube and collect with ASAP 2020, and the sample was vacuumed at 120 ℃ for 10 hours. After the sample cooling down, the water vapor was induced into the sample until the pressure reach to 4.12 $\times 10^{-3}$ bar at 298 K. The crystals were picked out and covered with the degassed oil in the glove box after 1 hour for single crystal X-ray diffraction measurements.

2.7 Preparation of water-loaded Cu-TDPAT at 3.01 $\times 10^{-2}$ bar (Cu-TDPAT-H$_2$O-2)

The selected anhydrous Cu-TDPAT was filled into a glass tube and collect with ASAP 2020, and the sample was vacuumed at 120 ℃ for 10 hours. After the sample cooling down, the water vapor was induced into the sample until the pressure reach to 3.01 $\times 10^{-2}$ bar at 298 K. The crystals were picked out and covered with the degassed oil in the glove box after 1 hour for single crystal X-ray diffraction measurements.

3. Density Functional Theory Calculations

Idealized Cu paddle-wheels linked by formate were built as representative model complex. Structural optimizations were performed by Gaussian 09 D.01[S3] using B3LYP hybrid functional with 6-31G* basis set[S4] for C, H, O atoms and Lanl2dz[S5] for Cu. Frequency calculations at the same level were calculated to verify either local minima or transition states and to estimate the thermal corrections Gibbs free energy at 298 K. To take water solvation effect into account, optimizations and frequency calculations under polarizable continuum model (PCM) were also performed with water as solvent.

**4. Single-crystal X-ray diffraction crystallography**

The single-crystal diffraction data were collected on a Bruker D8-Quest single-crystal diffractometer equipped with a CCD detector. The radiation source utilized was Mo Kα radiation (λ = 0.71073 Å) monochromated by a graphite monochromator, with an operating voltage of 50 kV and a current of 1 mA. Crystals, prepared beforehand, were encapsulated in crystal oil within a glovebox, and subsequently affixed to the apex of a glass fiber for testing on the diffractometer. The cell parameters refinement and

data reduction were performed using the program Bruker APEXII with absorption correction (multi-scan) applied.[S6] All the structures were solved by direct methods and refined anisotropically by full-matrix least-squares techniques based on F^2 using the SHELXS-97 and SHELXL-97 programs[S7] contained on Olex 2.[S8] Anisotropic thermal parameters were assigned to all non-hydrogen atoms. The hydrogen atoms of the ligand were generated geometrically; the hydrogen atoms of the water molecules were located in Fourier-difference electron density maps and refined with isotropic temperature factors. The large solvent accessible void in the lattice is caused by the vacuum process before single crystal diffraction measurement. Crystal data, as well as details of data collection and refinement for the complexes are summarized in Table S1. The X-ray crystallographic coordinates for structures reported in this study have been deposited at the Cambridge Crystallographic Data Centre (CCDC). The CCDC numbers for three compounds are 2365903 (Cu-TDPAT-H_2O-2), 2365904 (Cu-TDPAT-H_2O-1), 2365905 (hydrated Cu-TDPAT) respectively. These data can be obtained free of charge from the Cambridge Crystallographic Data Centre via www.ccdc.cam.ac.uk/data_ request/cif.
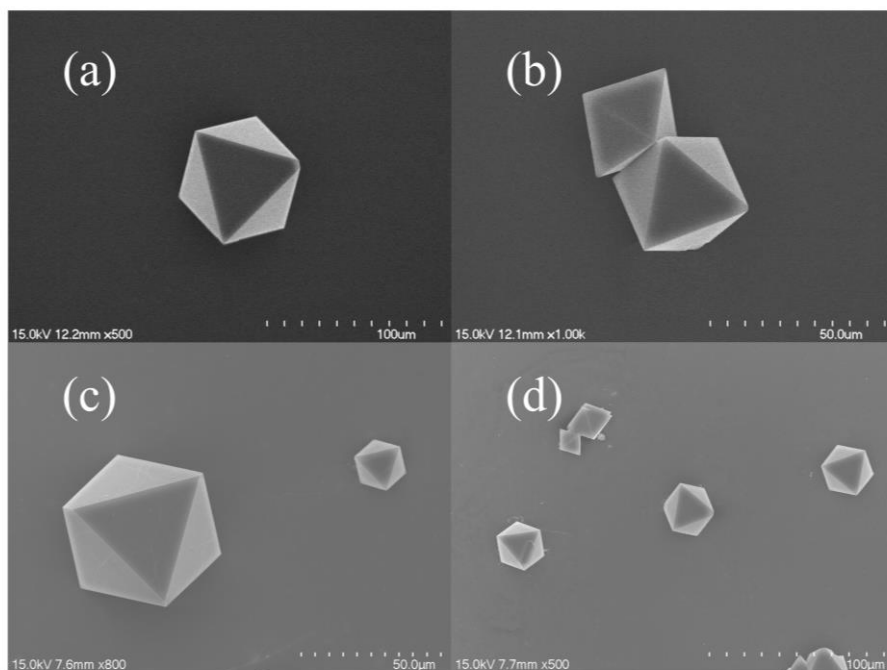
5. Supporting Figures and Tables
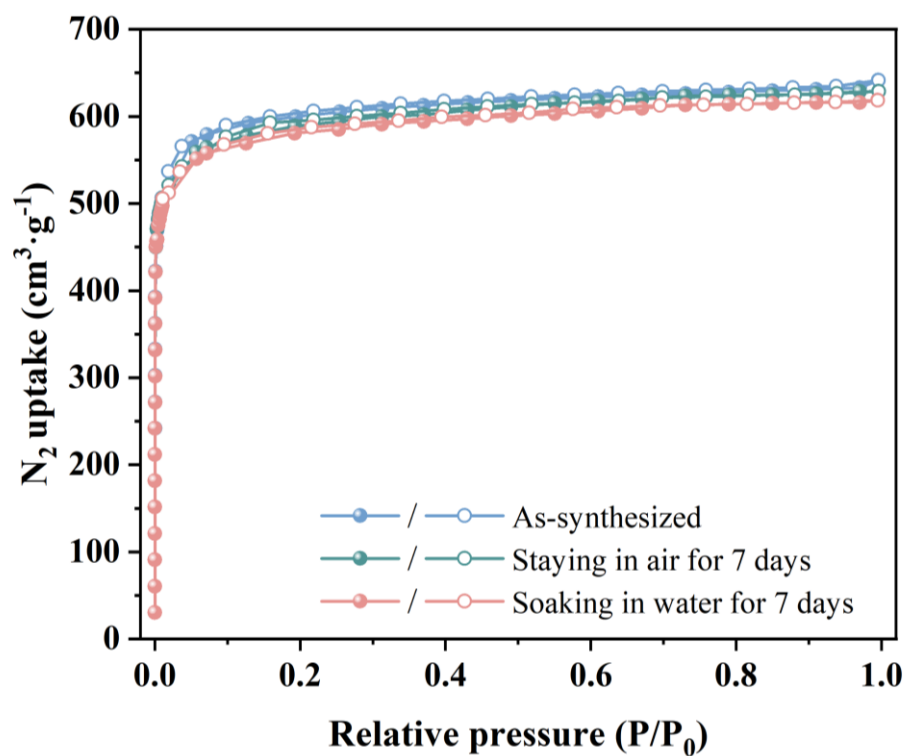
Figure S1 N_2 adsorption isotherms at 77 K of as-synthesized Cu-TDPAT and Cu-TDPAT samples after being treated in air for 7 days and in water for 7 days.
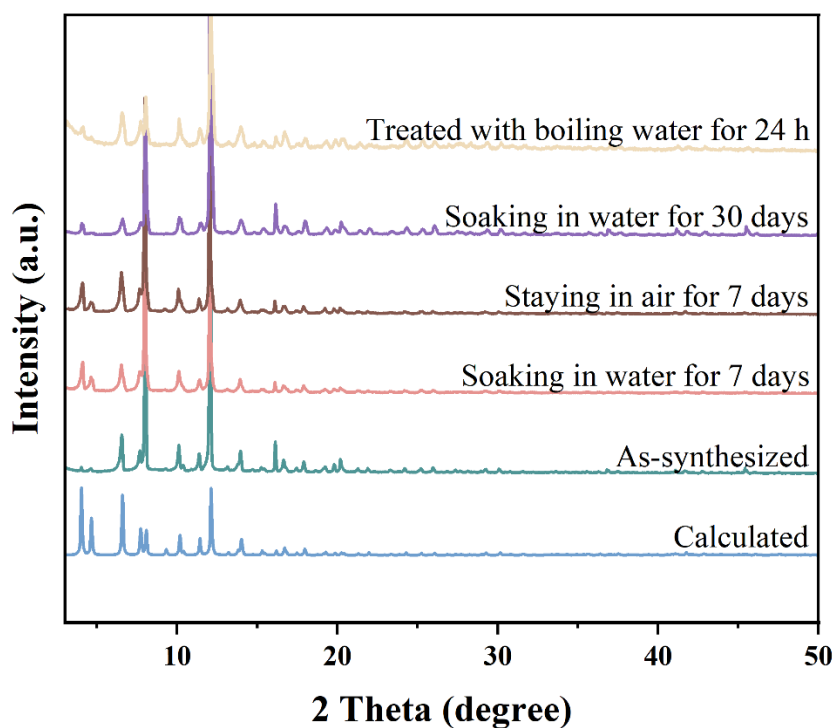
Figure S2 PXRD patterns for calculated, as-synthesized Cu-TDPAT, and Cu-TDPAT samples treated under different conditions.
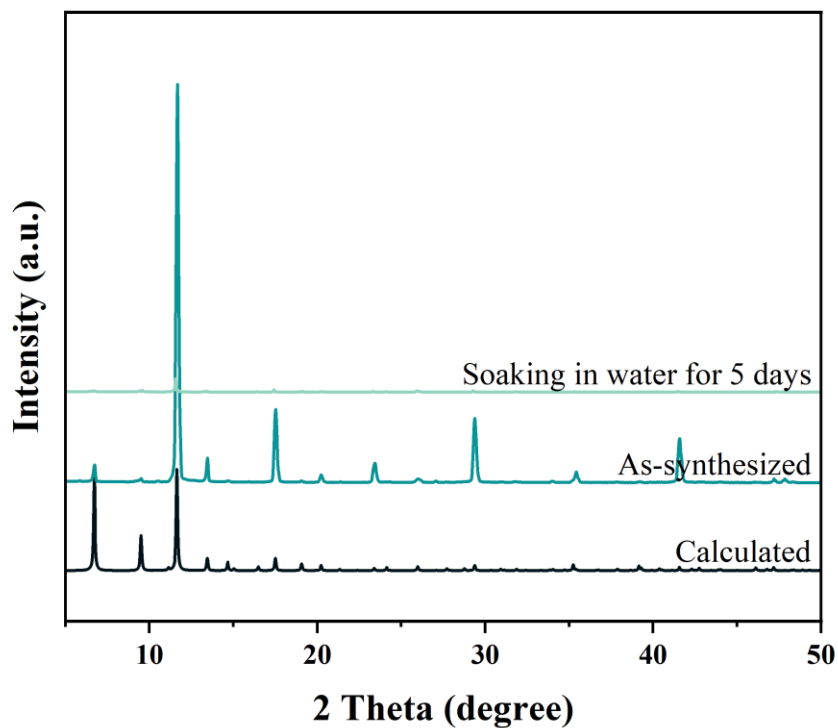
Figure S3 Scanning electron microscope (SEM) images of Cu-TDPAT crystal under different conditions. (a) (b) Pristine Cu-TDPAT crystals. (c) (d) Cu-TDPAT crystals were treated with water for 7 days.
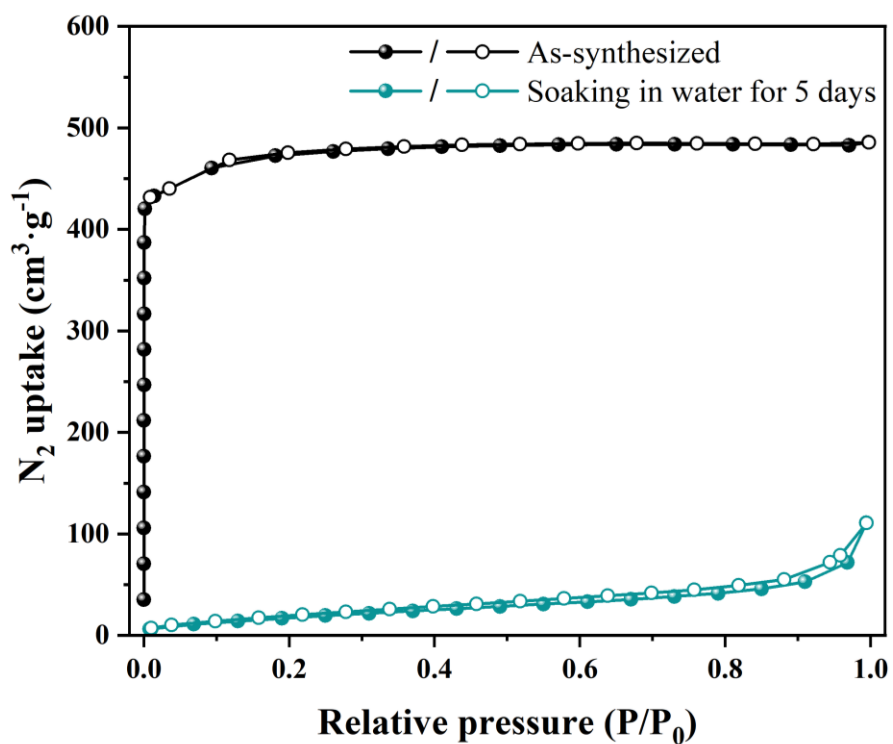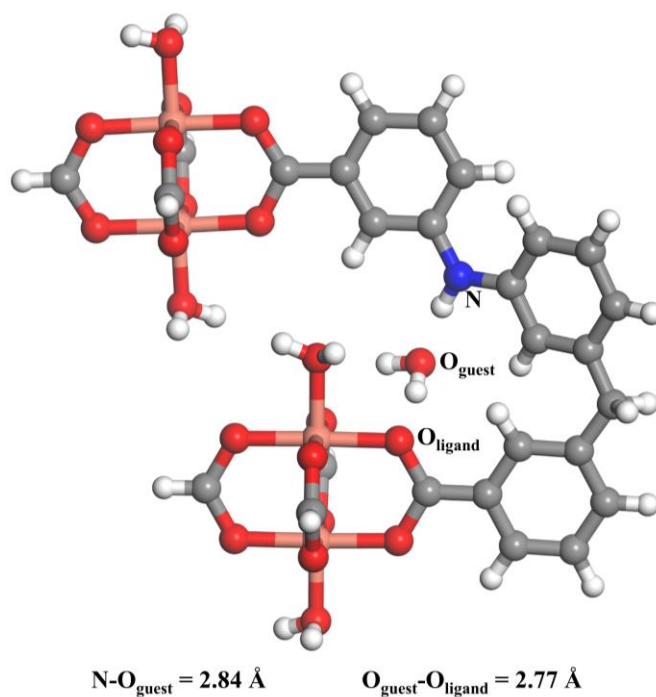

Figure S4 N_2 adsorption isotherms at 77 K of as-synthesized HKUST-1 and HKUST-1 samples after being treated in water for 5 days.
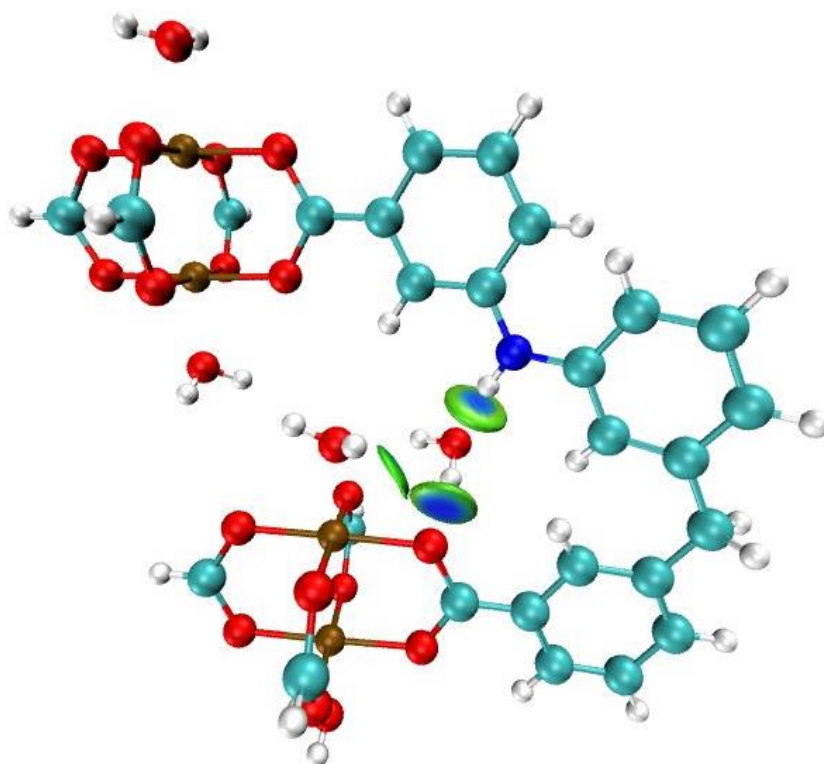
Figure S5 PXRD patterns for calculated, as-synthesized HKUST-1, and HKUST-1 samples treated in water for 5 days.

N-O$_{guest}$ = 2.84 Å   O$_{guest}$-O$_{ligand}$ = 2.77 Å

Figure S6 The hydrogen bonding distances between guest water molecule and the framework in hydrated Cu-TDPAT simulated by DFT calculations.

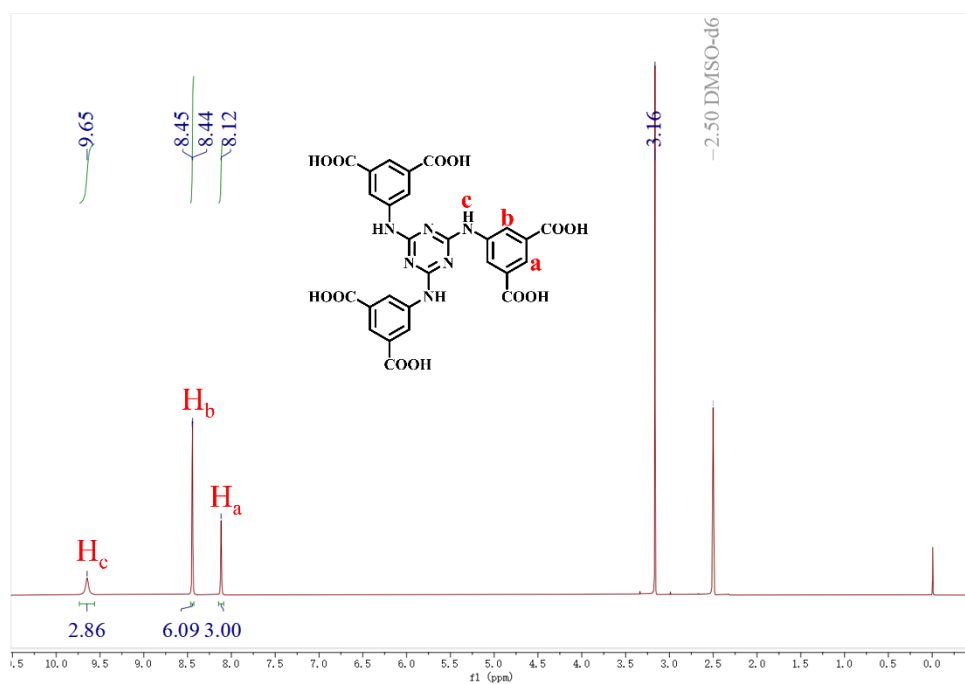**Figure S7** Sign(λ_2)ρ colored isosurfaces of $\delta g^{inter} = 0.007$ a.u. corresponding to IGMH analyses for water-loaded hydrated Cu-TDPAT.
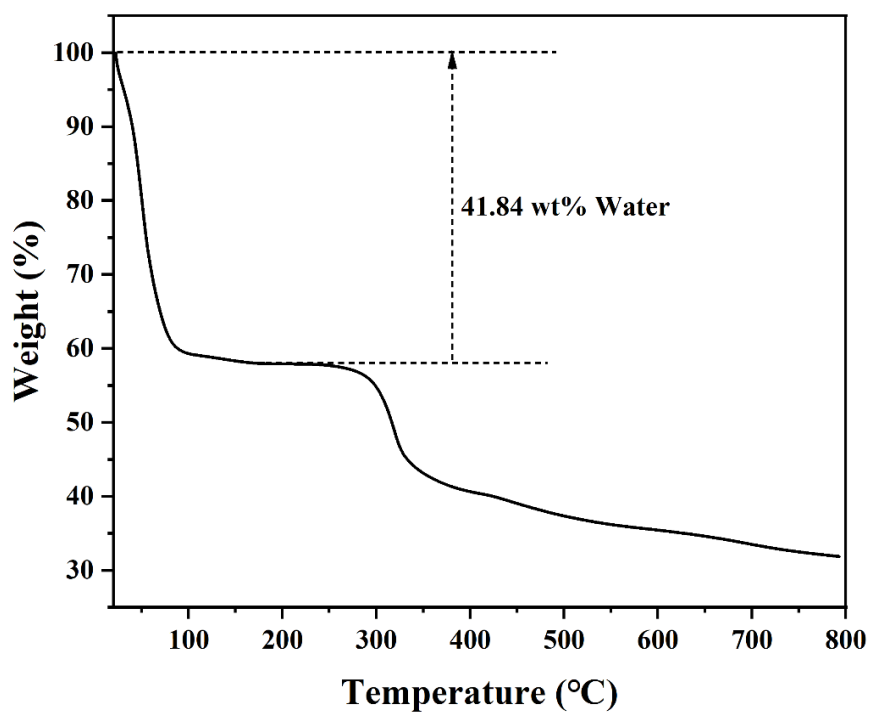
Figure S8 The TGA curve of Cu-TDPAT in N_2 atmosphere from room temperature to 800 ℃.
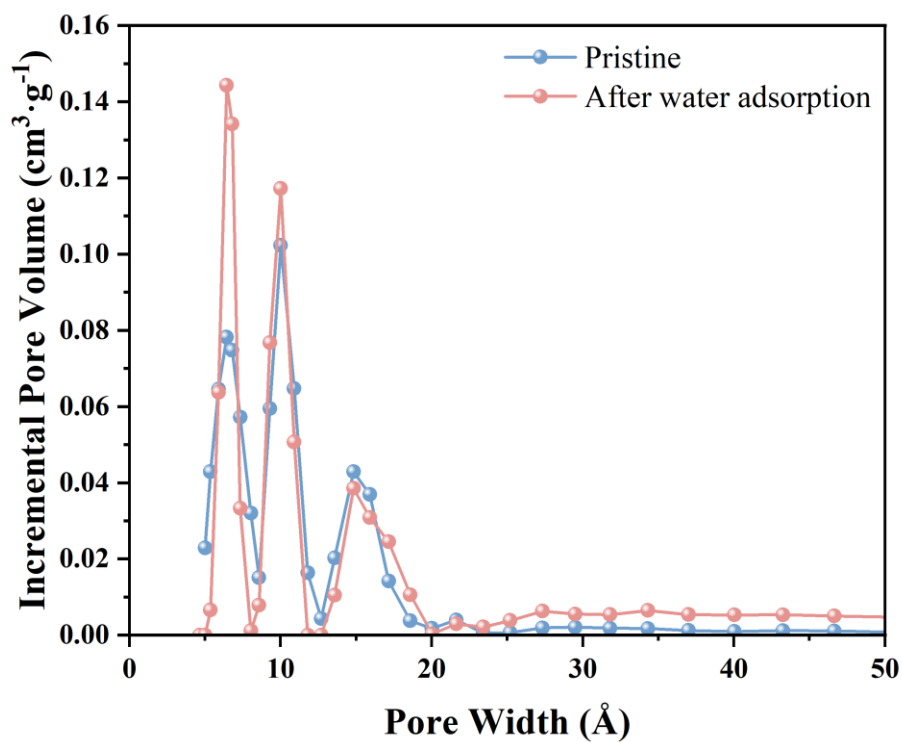
Table S1 Crystal data and structure refinement parameters for hydrated Cu-TDPAT, Cu-TDPAT-H₂O-1 and Cu-TDPAT-H₂O-2.

Compounds	hydrated Cu-TDPAT	Cu-TDPAT-H₂O-1	Cu-TDPAT-H₂O-2
Empirical formula	$C_{27}H_{14}Cu_3N_6O_{13}$	$C_{108}H_{121.64}Cu_{12}N_{24}O_{84.82}$	$C_{216}H_{512}Cu_{24}N_{48}O_{304}$
Formula weight	821.06	3875.53	10171.67
Temperature/K	150	150	150
Crystal system	Tetragonal	Tetragonal	Tetragonal
Space group	$I4/m$	$I4/m$	$I4/m$
a/Å	26.5844(17)	26.7494(6)	26.5441(12)
b/Å	26.5844(17)	26.7494(6)	26.5441(12)
c/Å	38.103(4)	38.4189(15)	37.881(2)
α/°	90	90	90
β/°	90	90	90
γ/°	90	90	90
Volume/Å³	26928(4)	27489.9(16)	26690(3)
Z	16	4	2
ρ_{calc} g/cm^{-3}	0.810	0.936	1.266
μ/mm^{-1}	0.974	0.971	1.034
F (000)	6544.0	7857.0	10544.0
Radiation	MoKα ($\lambda = 0.71073$)	MoKα ($\lambda = 0.71073$)	MoKα ($\lambda = 0.71073$)
2θ range for data collection/ °	4.846 to 49.996	4.69 to 50.056	4.34 to 52.782
Index ranges	$-31 \le h \le 23$ $-28 \le k \le 31$ $-45 \le l \le 45$	$-31 \le h \le 30$ $-31 \le k \le 28$ $-45 \le l \le 45$	$-25 \le h \le 33$ $-33 \le k \le 33$ $-41 \le l \le 47$

Goodness-of-fit on F^2	1.053	1.057	1.070
Final R indexes [$I \geqslant 2\sigma$ (I)]	$R_1 = 0.0423$ $wR_2 = 0.1194$	$R_1 = 0.0473$ $wR_2 = 0.1268$	$R_1 = 0.0597$ $wR_2 = 0.1729$
Final R indexes [all data]	$R_1 = 0.0519$ $wR_2 = 0.1252$	$R_1 = 0.0585$ $wR_2 = 0.1353$	$R_1 = 0.0758$ $wR_2 = 0.1865$
Largest diff. peak/hole/e Å^{-3}	0.63/-1.29	1.16/-0.47	1.22/-0.93

Table S2 Experimental values of hydrogen bond distances between heteroatoms in water-loaded Cu-TDPAT.

Hydrogen bonding distances between heteroatoms	Experimental values
O_G-N	3.10 Å
O_G-O_L	2.77 Å
O_G-O_C	2.74 Å
O_{21}-N_3	3.13 Å
O_{21}-O_6	3.09 Å
O_{21}-O_1	2.85 Å

6. References

1   B. Li, Z. Zhang, Y. Li, K. Yao, Y. Zhu, Z. Deng, F. Yang, X. Zhou, G. Li, H. Wu, N. Nijem, Y. J. Chabal, Z. Lai, Y. Han, Z. Shi, S. Feng, J. Li, *Angew. Chem. Int. Ed.* 2012, **51**, 1412-1415.

2   M. Ding, H.-L. Jiang, *CCS Chem.* 2021, **3**, 2740-2748.

3   M. Frisch, G. W. Trucks, H. B. Schlegel, G. E. Scuseria, M. A. Robb, J. R. Cheeseman, G. Scalmani, V. Barone, B. Mennucci and G. Petersson, *Journal*, 2009.

4   S. Grimme, J. Antony, S. Ehrlich and H. Krieg, J. *Chem. Phys*. 2010, **132**, 154104.

5   a) P. J. Hay, W. R. Wadt, L. R. Kahn and F. W. Bobrowicz, J. *Chem. Phys*. 1978, **69**, 984-997; b) W. R. Wadt, P. J. Hay and L. R. Kahn, J. *Chem. Phys*. 1978, **68**, 1752-1759; c) P. J. Hay and W. R. Wadt, J. *Chem. Phys*. 1985, **82**, 299-310.

6   A. Dawson, D. R. Allan, S. Parsons, M. Ruf, *J. Appl. Crystallogr.* 2004, **37**, 410-416.

7   G. M. Sheldrick, *Acta Crystallogr. Sect. C-Struct. Chem.* 2015, **71**, 3-8.

8   J. Lübben, C. M. Wandtke, C. B. Hübschle, M. Ruf, G. M. Sheldrick, B. Dittrich, *Acta Crystallogr A.* 2019, **75**, 50-62.